DYNA
ISSN: 0012-7353
Universidad Nacional de Colombia

Castrillón-Restrepo, Juan Pablo; Jiménez-Gómez, Sebastián; Saldarriaga-Ángel, Federico
Development of a parametric cable driven planar robot
DYNA, vol. 85, no. 206, 2018, July-September, pp. 49-58
Universidad Nacional de Colombia

DOI: https://doi.org/10.15446/dyna.v85n206.69233

UNIVERSIDAD NACIONAL DE COLOMBIA
SEDE MEDELLÍN
FACULTAD DE MINAS

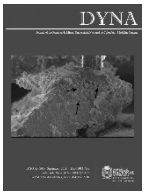

DYNA
http://dyna.medellin.unal.edu.co/

Development of a parametric cable driven planar robot

Juan Pablo Castrillón-Restrepo, Sebastián Jiménez-Gómez & Federico Saldarriaga-Ángel

Universidad EIA, Envigado, Colombia. juan.castrillon21@eia.edu.co, sebastian.jimenez1@eia.edu.co, federico.saldarriaga@eia.du.edu.co

Received: December 5th, de 2017. Received in revised form: May 5th, 2018. Accepted: July 24th, 2018

Abstract
Cable driven robots have been a widely researched topic in the last few years, this is due to the advantages that they present over conventional parallel robots. In this paper, all the areas of robotic design have been studied for a planar cable driven robot, with the objective of making it parametric, meaning that the design process and mathematical models used in this paper could be used to implement the suggested architecture to solve any specific need. Finally, using the parametric design approach, a prototype was developed and built in order to validate the design process, evaluate the robot's precision, identify future works and improvements and foresee any trouble that was not considered during the design phase.

Keywords: cable driven parallel robots; kinematics; feasible workspace; control systems; trajectory tracking.

Desarrollo de un robot cartesiano parametrizable comandado por cables

Resumen
Los robots comandados mediante cables han sido muy estudiados en los últimos años, debido a las ventajas que presentan con respecto a otros robots paralelos. En este trabajo, se estudian todas las áreas del diseño robótico para un robot por cables planar cuyo objetivo principal es ser parametrizable, es decir, que el proceso de diseño y los modelos matemáticos utilizados en este trabajo se puedan escalar fácilmente permitiendo implementar la arquitectura trabajada para necesidades específicas. Finalmente, usando el diseño paramétrico, se desarrolló y construyó un prototipo con el fin de validar el proceso de diseño y evaluar precisión en su movimiento, así como identificar futuras mejoras y prever puntos críticos tanto en el diseño mecánico como en los sistemas de actuación no consideradas en el proceso de diseño.

Palabras clave: robot comandado mediante cables; cinemática; espacio de trabajo alcanzable; sistemas de control; seguimiento trayectoria.

1. Introduction

Cable Driven Parallel Robots or CDPR have been widely studied in many areas. For uses such as Contour Crafting [1]] to manipulate patients in medical areas [2], these types of robots are versatile in many applications [3]. Therefore, CDPR are ideal for pick and place operations [4] due to their high speeds and large workspaces. Compared to rigid parallel manipulators, cable-driven parallel robots use cables as links instead of rigid ones to control the motion of the end-effector. CDPR provide desirable characteristics, including potential large workspace, the facility to be reconfigured, high speeds of motion, and high payload capacities to weight ratios [5]. Additionally, CDPR with small to very large cable lengths allow them to be stored on spools or drums thus allowing to build robots with a workspace of wide dimension. Depending on their size they may be less expensive, easier to build, reconfigured, safer and non-invasive [6].

The following paper takes a parametric approach on the design process of CDPR, highlighting one of the main advantages of these types of robots that is scalability. In order to validate and foresee possible errors in this approach, a prototype was developed and tested. Subsequently, the paper details the design and construction process for a suspended planar cable robot starting with the relevant mathematical models shown in section 2. Based on the models, a graphic interface was programed to be able to select the actuators needed for any suspended planar robot to be built, making its design parametric. Section 3 shows

How to cite: Castrillón-Restrepo, J.P., Jiménez-Gómez, S. and Saldarriaga-Ángel, F., Development of a parametric cable driven planar robot. DYNA, 85(206), pp. 49-58, September, 2018.

the interface and the mechanical, electronic and control design and implementation for a built prototype.

Finally, section 4 presents the measurement results of the said prototype's movements comparing simulations and experimental results in order to validate the design process. Conclusions are shown in the last section for future projects and recommendations for the construction process.

2. Models

Within CDPR, different architectures are identified and can be classified according to [7] in the following ways:

According to their degrees of freedom:

- Planar: They can move and turn in a single plane (2 dimensions)
- Spatial: Allow movement and orientation changes in a three-dimensional space

Depending on the connection between the cables and the end effector:

- Suspended: Constructed so that the vertical components of the tensions in the cables are always opposite to the force of gravity
- Commanded: A robot is considered commanded when some of the components of the cable tensions go in the same direction as gravity

Depending on the number of cables in the system:

- Under-Constrained: When the end effector has infinite positions or orientations for certain lengths of its cables
- Fully-constrained: When, through a combination of cable lengths, the end-effector can find only a single position or orientation
- Over-Constrained: When a single position or orientation can be reached through different cable configurations.

Mathematical models are defined to study robotic cable systems cables. These models vary depending on the architecture selected. This article focuses on a planar suspended robot and will then expose its relevant mathematical models: Inverse kinematics, static and velocity analysis.

2.1. Inverse kinematics

In a robot, kinematics is defined as the relationship between the position and orientation of its end effector with its articular coordinates [8]. In this way, the inverse kinematics allow to obtain the value to be taken by the actuators to achieve a specific position and orientation of the robot`s end.

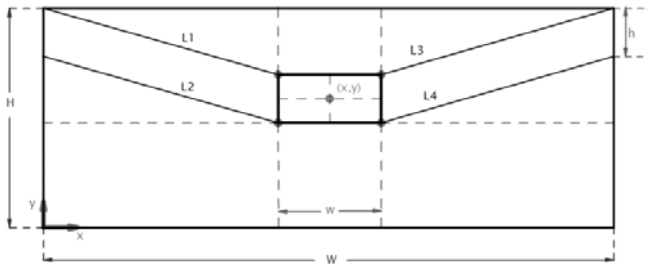

Figure 1. Representation of a suspended CDPR
Source: Authors

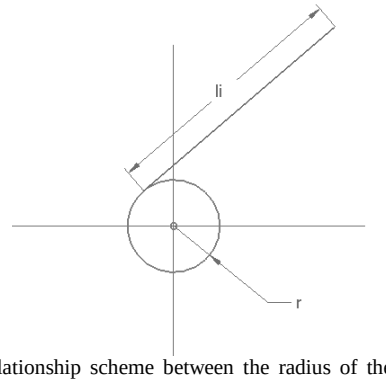

Figure 2. Relationship scheme between the radius of the pulley and the length of the cable
Source: Authors

In the specific case of the CDPR, the inverse kinematics aim to find the lengths of the cables for a certain position of the end-effector. In Fig. 1, a simplified scheme of the implemented architecture is presented:

Geometric relationships are found between the length of the cables (L1, L2, L3 and L4) and the position of the end effector as shown in the equations found at (1)):

$$\begin{aligned} L1_x = x - \frac{w}{2} \;;\; L1_y = H - \left(y + \frac{h}{2}\right) \\ L3_x = W - (x + \frac{w}{2}); L3_y \\ = H - \left(y + \frac{h}{2}\right) \\ Li_{total} = \sqrt{{li_x}^2 + {li_y}^2} \\ L1_{total} = \quad L2_{total} \\ L3_{total} = \quad L4_{total} \end{aligned} \tag{1}$$

Finally, the lengths with the articular coordinates are related making use of the diagram in Fig. 2 and the equation (2).

$$\begin{aligned} \Delta L_i = r * q_i \;\; where\, \Delta L_i \\ = l_{i-actual} - l_{i-desired} \\ q_i = \frac{\Delta L_i}{r} \end{aligned} \tag{2}$$

2.2. Static analysis

In cable driven parallel robots, the work space is limited, not only by the dimensions of the frame, but also by the tension present in each of the cables in a given instant [3]. Therefore, the workspace area of a CDPR is defined by the space within the frame whose Cartesian coordinates ensure that the tension has a positive value in all of its cables. If α is

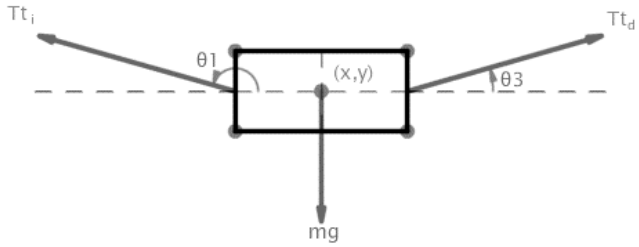

Figure 3. FBD simplification for the suspended cable driven robot
Source: Authors

defined as the set of the points that belong to the workspace, Equation (3) summarizes this definition in the following expression:

$$T(x,y) > 0 \rightarrow (x,y) \in \alpha \tag{3}$$

When defining Tt_i as the sum of tensions on the left side and Tt_d as the sum of tensions on the right side, the tensions can be simplified using a free body diagram (FBD) as shown in the Fig. 3.

By means of geometric relations, the values for the angles of the tensions can be expressed as in Equation (4).

$$\theta_1 = \pi - \tan^{-1}\left(\frac{H-(y+\frac{h}{2})}{x-\frac{w}{2}}\right)$$
$$\theta_3 = \tan^{-1}\left(\frac{H-(y+\frac{h}{2})}{W-(x+\frac{w}{2})}\right) \tag{4}$$

Establishing equilibrium equations ($\sum F_x = 0; \sum F_y = 0$), the Jacobian matrix ($A$) can be obtained and the independent term vector (b) shown in Equation (5).

$$\boldsymbol{A} = \begin{bmatrix} \cos(\theta_1) & \cos(\theta_3) \\ \text{sen}(\theta_1) & \text{sen}(\theta_3) \end{bmatrix}$$
$$\boldsymbol{b} = \begin{bmatrix} 0 \\ mg \end{bmatrix} \tag{5}$$

Lastly, to identify the tensions in the cables, the solution for the equation system is described as follows:

$$\boldsymbol{T} = \begin{bmatrix} Tt_i \\ Tt_d \end{bmatrix} = \boldsymbol{A^{-1}} * \boldsymbol{b} \tag{6}$$

It is then possible to generate the achievable workspace of this type of robots using a computational tool like *Matlab* ®. The result is shown in Fig. 44.

In reality, there are factors that modify the shape of this workspace; factors such as the minimum tension and the maximum tension allowed by the actuators. The evaluation of the effects of these factors on the workspace are observed in Fig. 5 and Fig. 6 respectively.

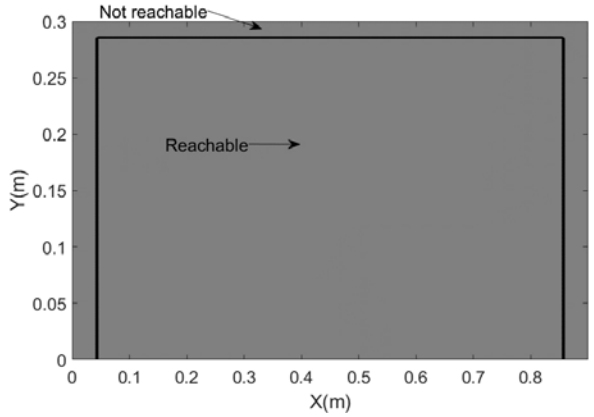

Figure Ideal workspace for a CDPR
Source: Authors.

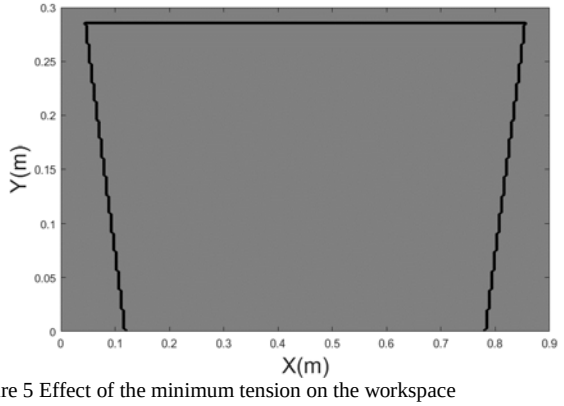

Figure 5 Effect of the minimum tension on the workspace
Source: Authors.

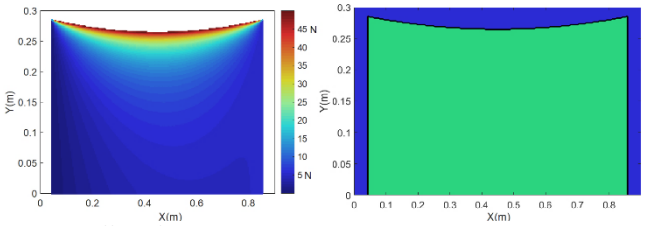

Figure 6. Effect of the maximum tension on the workspace
Source: Authors.

2.3. Velocity analysis

For the speed analysis of the robot, the mathematical model used was the inverse Jacobian matrix. This allows to obtain the speeds of the articulations of the Robot (actuators) starting from speeds defined for the edge [8]:

$$\begin{bmatrix} \dot{q_1} \\ \dot{q_2} \end{bmatrix} = \boldsymbol{J^{-1}} * \begin{bmatrix} \dot{x} \\ \dot{y} \end{bmatrix} \tag{7}$$

Starting from the equations (1) and (2) that describe the inverse kinematics, they can be derived in time and using eq.(7), the inverse Jacobian matrix is defined as shown in (8).

$$\dot{q}_i = \frac{dq_i}{dt} = \frac{dL_i}{dt} * \frac{1}{r} \qquad where\ r = pulleys\ radius$$

$$\begin{bmatrix} \dot{q_1} \\ \dot{q_2} \end{bmatrix} = \begin{bmatrix} \frac{x-w}{L_1 * r} & \frac{y+h-H}{L_1 * r} \\ \frac{x+w-W}{L_2 * r} & \frac{y+h-H}{L_2 * r} \end{bmatrix} * \begin{bmatrix} \dot{x} \\ \dot{y} \end{bmatrix} \quad (8)$$

3. Tools and methods

3.1. Parametric design

Based on the mathematical models explained in the previous section, aiming to develop a parametric system, a program was developed in order to select the actuators required for the construction of any CDPR with the mentioned architecture (planar suspended). Specifying needs of space and load of the robot, the interface also needs the following parameters as entrees for the calculus:

- Height: Vertical dimension of the desired work space and the end effector in meters.
- Payload: Mass in kg to be manipulated by the robot.
- Dimension factor: A factor that relates how large the frame in regar• Length: Horizontal dimension of the desired working space and the end effector in meters
- ds to the desired workspace of the robot (must be greater than 1)
- Minimum tension safety Factor: Percentage of the mass equal to the minimum tension of the robot. This factor guaranties that the tension in the cables is never equal to zero or negative values; therefore, the robot never loses orientation of the end effector.
- Pulley Radius: Radius of the pulleys carrying the actuators.
- X: presents two spaces to enter the initial and final position of the effector in the x-coordinate, in order to calculate the speeds.
- Y: Presents two spaces to enter the initial and final position of the effector in the y-coordinate, in order to calculate the speeds.
- T: time to perform the movement established in the previous entries.

As output parameters, the interface is capable of calculating the minimum torque required, the maximum velocities and the power of the motors or actuators needed for the robot. The interface can be seen in Fig. 7:

Using the developed program, actuators were calculated to create a prototype. It was determined that the robot to be built will handle a load of 1 kg and reach maximum vertical speeds of 20 cm/s. So, the input and output parameters are seen in Table 1 and Table 2 respectively:

3.2. Mechanical system

Once the requirements of the actuators are obtained, the characteristics of the chosen motors are seen in Table 3 [9].

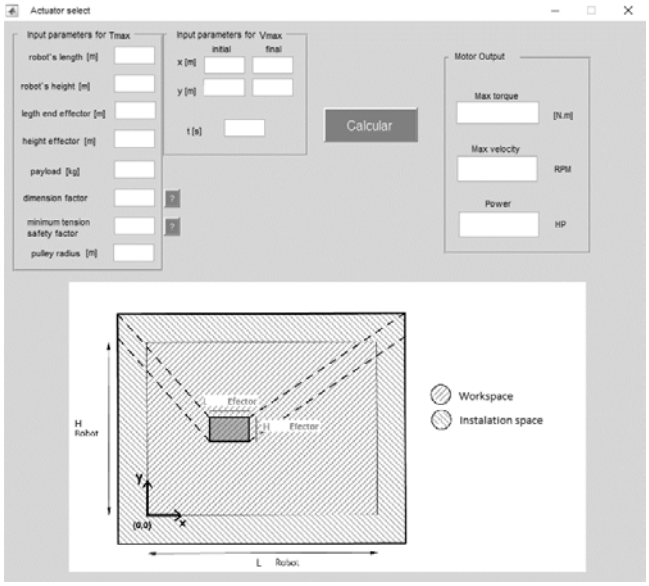

Figure 7. Program interface for the selection of actuators
Source: Authors.

Table 1.
Entre parameters for the user interface

Parameter	Value
Length of the Robot	0.9 m
Height of the Robot	0.3 m
Length of effector	0.12 m
Height of effector	0.04 m
Payload	1 kg
Dimension factor	1.42
Minimum tension safety factor	0.1
Pulley Radius	0.05 m
X Initial	0.45 m
X final	0.45 m
Y initial	0.3 m
Y final	0.1 m
t	1 s

Source: Authors.

Table 2.
Parameters given by the user interface

Output	Value
Minimum torque required	1.3741 Nm
Maximum velocity	16.7119 RPM
Power	0.003224 HP

Source: Authors.

Table 3.
Parameters for the motor used in the prototype

Specifications of the Motor POL1445	
Size	37D x 66L (mm)
Weigh	220g
Shaft diameter	6mm
Transmission relationship	70:1
Free rotation speed @ 12V	150 rpm
Free rotation current @ 12V	300 mA
Stall current	5 A
Stall torque	200 oz-in(1.42 N.m)

Source: Authors.

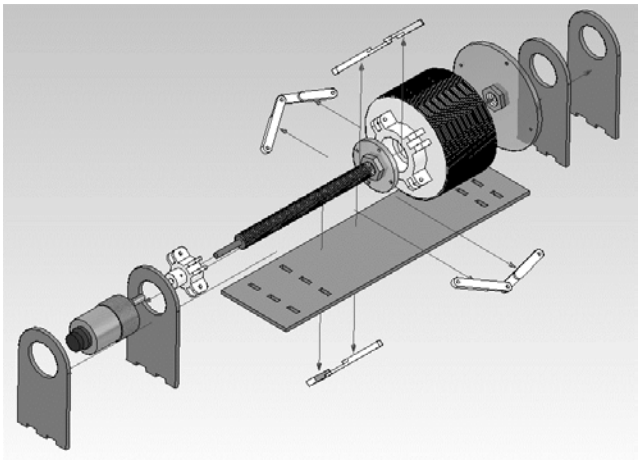

Figure 8 Mechanism to wind the cable
Source: Authors.

Once the actuators were chosen, it was necessary to develop a mechanical system that allowed the cable to be rolled and released. A mechanical system was implemented to ensure that the pulley radius did not change, and the alignment of the cable remained constant. To avoid distorting forces in the end effector movement, a solution was based on [10] and modified to adapt to the specific needs of the prototype.

The mechanism is a threaded drum or pulley, where the cable winds up. This drum spins in a fixed threaded shaft to ensure the same starting point for any instance of time. The details of the adapted mechanism are seen in Fig. 8.

The next elements in the robot's mechanical system are the upper pulleys. These allow the cables to have opposite tensions to gravity, even if the actuators are positioned at ground level. Their design was made in order to eliminate any perpendicular forces to the motion plane of the robot, as well as unwanted output angles. For this reason, they were designed with a minimum thickness so that only a nylon cable could pass between their inner faces (Fig. 9).

Finally, the end effector was designed so that the four cables could be secured ensuring that the distance between cables never changed, as shown in the Fig. 10.

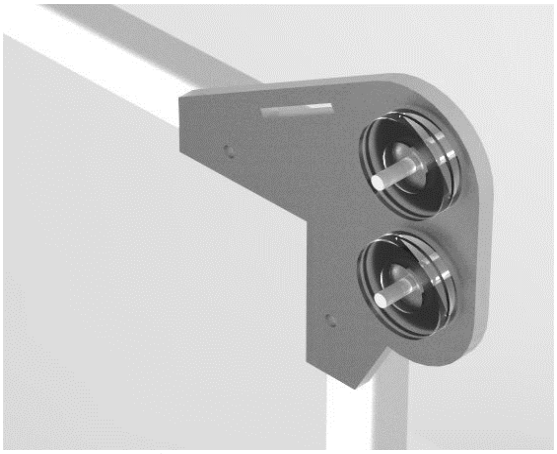

Figure 9. Top pulleys of the CDPR
Source: Authors.

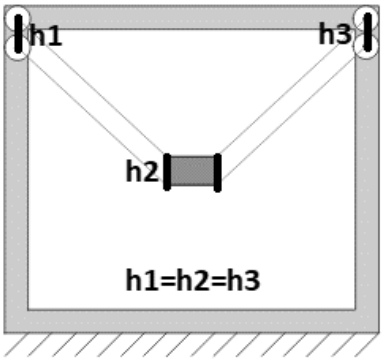

Figure 10. Illustration for equal lengths between cables.
Source: Authors.

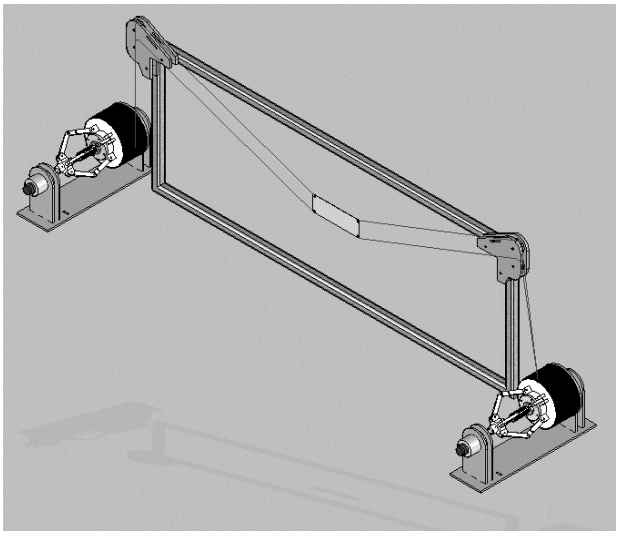

Figure 11 Mechanic assembly of the CDPR
Source: Authors.

Fig. 11 shows the mechanic assembly of the CDPR.

3.3. Control system

To determine the position of the end effector in the robot, position controllers were tuned for the actuators and a decentralized design was implemented to enable perform synchronous tasks. This meaning, being able to perform movements on both motors simultaneously.

The tuning of these controllers starts with the identification of the system then a controller design process and a final performance evaluation [11].

3.3.1. System identification

To appropriately control the actuators, it is first necessary to identify system dynamics using a transfer function. To avoid the inherent destabilizing dynamics in the position of a dc motor, the angular velocity of the system had to be identified, and then proceed to find the position function, using the expression shown in equation (9).

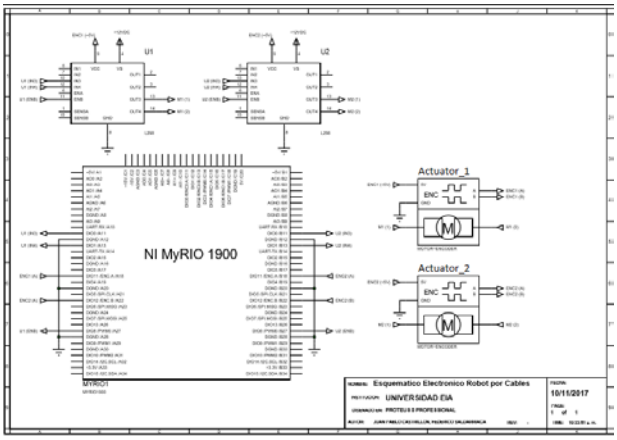

Figure 12. Connection diagram for identification and operation of the DC motors in the CDPR
Source: Authors.

$$\omega(t) = \frac{d\theta(t)}{dt} \rightarrow \omega(s) = \theta(s) * s \tag{9}$$

To identify the system, the motor was stimulated using step signals in PWM percentages and the response of its angular velocity was observed using the incremental Quadrature encoder integrated into the motor. For this, a National Instruments MyRIO acquisition board was used [12] and connected to the actuators as shown (Fig. 12).

Equation (10) shows the formula used to determine the angular velocity of the motor using position measuring elements such as quadrature encoders:

$$\omega\ (rpm) = \frac{\frac{encoder\ pulses\ (process\ output)}{ppr(4480)} * \frac{60\ s}{1\ min}}{sample\ time\ _{(s)}(0.01)} \tag{10}$$

It is necessary to mention that this measurement is possible given the good resolution of the encoders and the acquisition board. Otherwise this identification strategy would not be feasible.

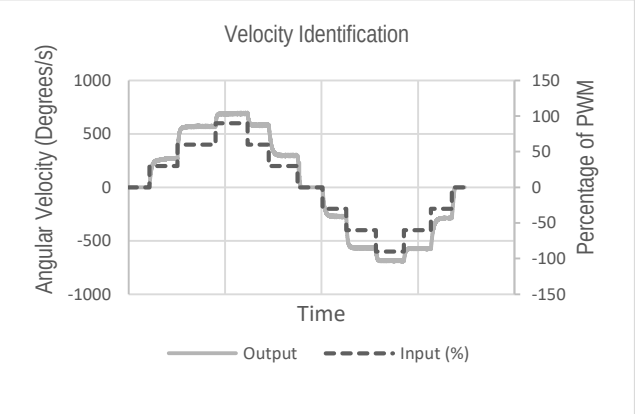

Figure 13. Identification process
Source: Authors.

Table 4.
Tuned controllers for the actuators

Controller	Equation	P	I	D	N
PID	$P + \frac{I}{s} + \frac{D * N}{1 + \frac{N}{s}}$	0.277	0.00598	0.146	285.02
PI	$P + \frac{I}{s}$	0.0475	0.00034	X	X
PD	$P + \frac{DN}{1 + \frac{N}{s}}$	0.2964	X	0.155	304.8

Source: Authors.

The data obtained from the identification experiment is observed in Fig. 13.

The data shown in Fig. 13, was processed using the *Matlab*® identification toolbox which estimates a transfer function (*tf*) and evaluates its accuracy or fit using system data. With a fit of 88.61%, the transfer function obtained can be observed in eq. (11).

The parameters given for the identification process were 1 pole and no zeros in order to get the transfer function (11).

$$tf\ for\ velocity = \frac{17.18}{s + 1.933} \tag{11}$$

The mentioned fit is given by the program and calculated internally by the *Matlab*® identification toolbox [13].

Once the velocity transfer function was established, it was integrated to the time factor to obtain a position transfer function:

$$tf\ for\ position = \frac{17.18}{s^2 + 1.933s} \tag{12}$$

3.3.2. Controller design

Starting 3 main architectures of controllers (PID, PI and PD), these were designed with similar performance parameters to obtain a system with critically damped behavior (ζ=1). Using a sampling time of T=0.01 and settling times 1.5 and 4 seconds, the best controllers of each type were obtained and are described in Table 4.

3.3.3. Performance evaluation

Given the desired settling times and robustness parameters for the tuned controllers [14], a pattern signal was designed (Fig. 14) including sine-type dynamics given their smooth accelerations and ramp-type dynamics in order to obtain constant speeds and step-type references to evaluate their behavior to drastic changes in the reference. This signal tested the three designed controllers (Table 4).

Error metrics were used to evaluate controller performance by means of: ITAE and relative error, related in equations (13) and (14). Table 5 shows the comparison of the results for each controller. It is seen that for both performance parameters the controller PD had the best performance.

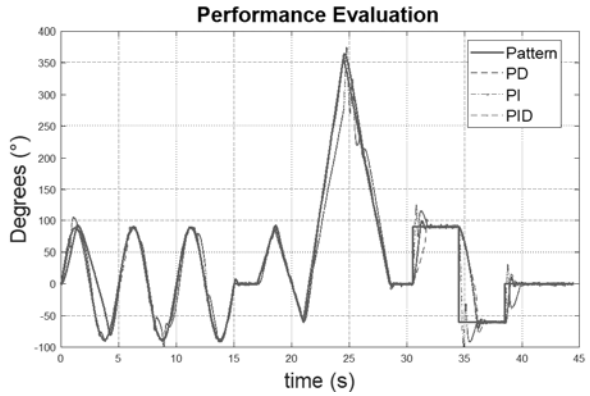

Figure 14. Pattern signal for controller evaluation
Source: Authors.

Table 5.
Controller performance to the pattern signal

Controller	ITAE	$\hat{e}$(%)
PD	8.905	12.501
PI	16.44	15.583
PID	21.68	32.8871

Source: Authors.

Considering the hardware used and its limitations, the error obtained for the PD controller is partially the result of having low specification hardware. Factors such as encoder resolution or gear backlash can greatly affect the controller performance [15]. Improving hardware specifications can resolve smaller errors as shown in [16].

$$ITAE = \int_{to}^{tf} t * |y(k) - \hat{y}(k)| dt \tag{13}$$

$$\hat{e} = \frac{1}{N} * \sum_{k=to}^{tf} \left| \frac{y(k) - \hat{y}(k)}{y(k)} \right| * 100 \tag{14}$$

It is important to consider that the error measured for each controller considers both transient and stable state dynamics. It is also generated by trying to follow an ideal trajectory, which represents the most critical conditions possible in terms of speed and acceleration for the robot's movement and position control system.

3.3.4. Motor synchronization

Because cable driven robots are parallel robots, trajectories of the end effector depend on how synchronized the robot actuators (motors) are. In other words, appropriate and adequate movement of the end effector, the initial and final times for the trajectory of the motors must be as similar as possible. This, not only guarantees the initial and final position of the effector, but also ensures linearity in the trajectories to be performed. To determine dual motor synchronization, an experiment was designed in which, the PD controller was implemented in both actuators and the pattern signal of both motors was measured to compare results.

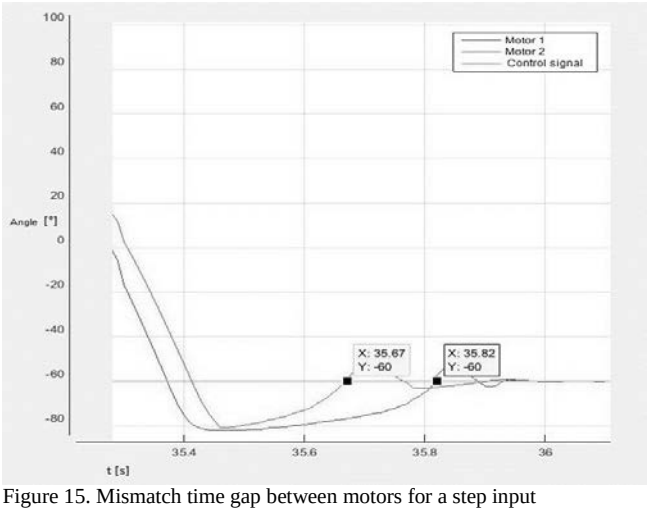

Figure 15. Mismatch time gap between motors for a step input
Source: Authors.

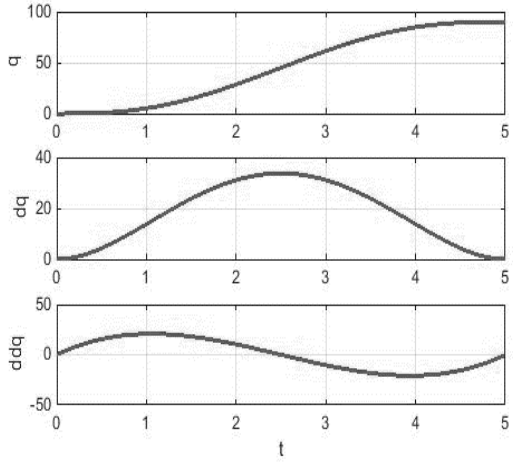

Figure 16. Fifth order trajectories
Source: Authors.

When measuring actuator behavior, the greatest time mismatch for the step type signals was of 0.2 seconds. An example of this behavior is shown in Fig. 15. This gap is considered acceptable because step signal dynamics will not be present in the robot, because as shown in the next section, soft polynomial trajectories were chosen as reference signals for the system.

3.3.5. Trajectory generation

In order to restrict actuator accelerations and speeds in all points of the trajectory, high order polynomial trajectories were selected [17]. From these trajectories, physical restrictions, precision criteria and softness were then contemplated [8]. Otherwise, "in the polynomial trajectories the degree of the polynomial depends on the number of conditions to be satisfied as well as of the smoothness in the resulting movement" [18] fifth-order trajectories were implemented, like those shown in Fig. 16.

Figure 17. Real prototype CDPR
Source: Authors.

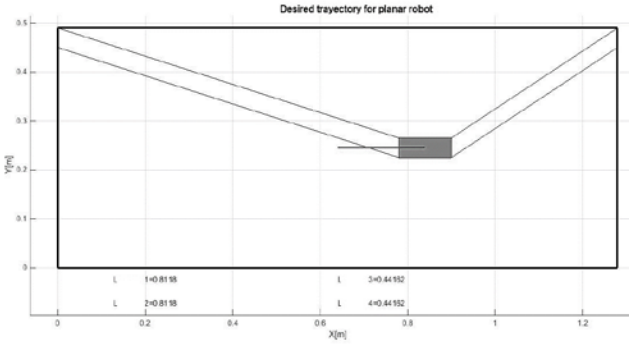

Figure 18. Horizontal trajectory
Source: Authors.

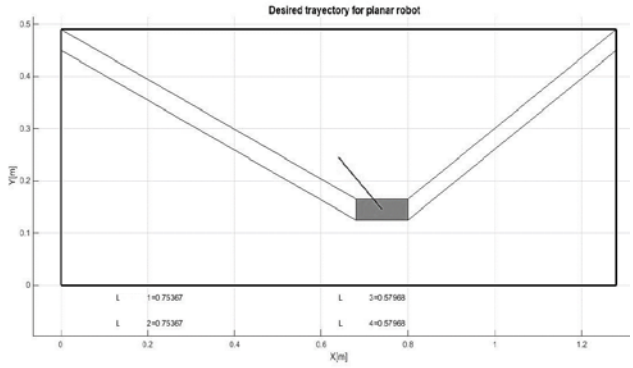

Figure 19. Diagonal trajectory
Source: Authors.

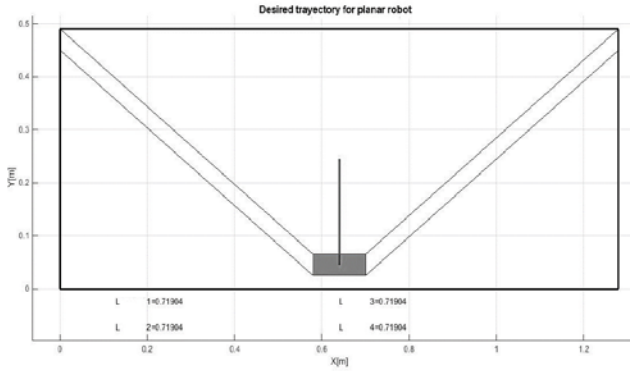

Figure 20Vertical trajectory
Source: Authors.

4. Results

The built robot can be seen in Fig. 17.

Once built, three Cartesian trajectories were designed to test its operation, which are seen in Fig. 18 through Fig. 20.In order to obtain displacement measurements for the end effector to determine the precision of the prototype, two different measurements were used: first, the trajectories in the motors were simulated without having the robot assembled and with the use of the direct kinematics of the robot, an approximate trajectory of the end effector was produced. Second, with the built robot and using the assembly shown in Fig. 21, a video of the robot`s movement was taken and analyzed with video analysis software. Measuring the end-effector position using computer vision, which has proven to be an adequate method that presents the advantage of demonstrating the effects of certain parameters such as the flexible nature of cables. Simultaneously, because it is an external measurement, system performance is not affected [6]. Tracker software works by measuring an object's displacement frame by frame to determine the actual movement of the object in the video [19]. This, to point out that the robot was recorded with a 60 FPS and 1080 p. camera.

Both results (simulation and real movement), as well as the desired trajectory, are showed in Fig. 22 through Fig. 24:

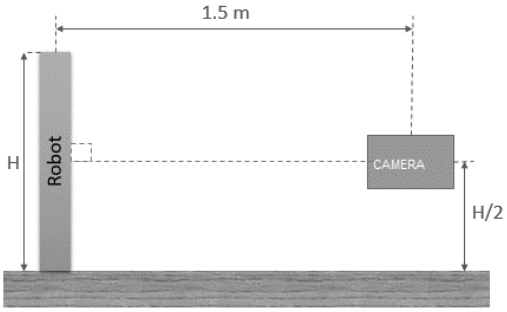

Figure 21. Setup used to record the movement of the robot
Source: Authors.

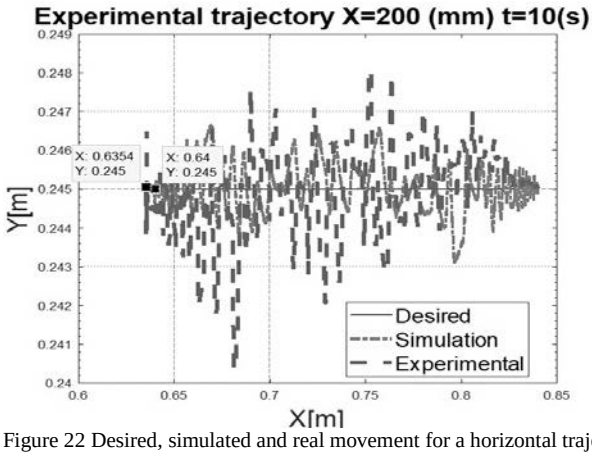

Figure 22 Desired, simulated and real movement for a horizontal trajectory of 20 cm
Source: Authors, 2018.

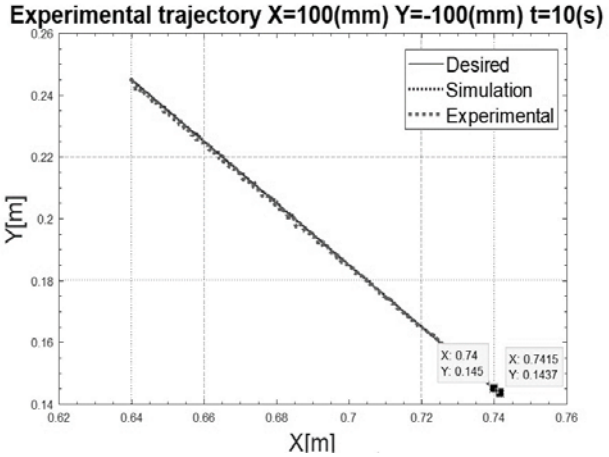

Figure 23. Desired, simulated and real movement for a diagonal trajectory of equal components (10 cm)
Source: Authors.

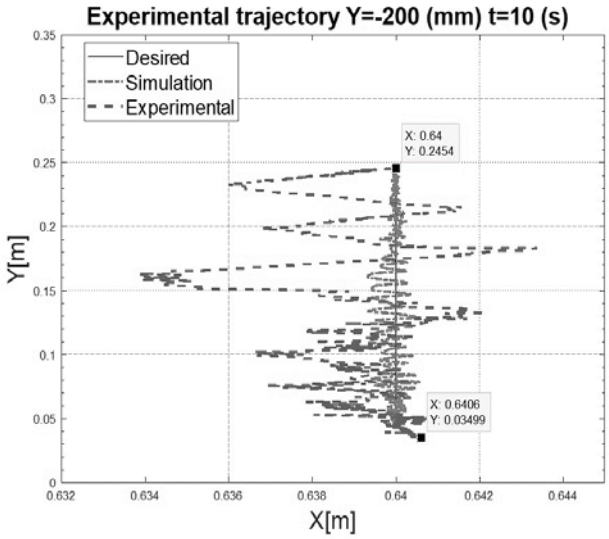

Figure 24. Desired, simulated and real movement for a vertical trajectory of 20 cm
Source: Authors.

In the previous figures, the blue trajectory is the desired, the red trajectory is the simulated using the encoder measurements and the direct kinematics model and the violet trajectory is measured with the non-invasive proposed method. The previous tests show that the maximum deviation for the built prototype was 3% for the trajectory of 200 mm in X.

Errors can be traced back to many factors of the prototype. On the other hand, hardware limitation influence in controller performance, explained in section 3.3.3, proves there are certain inherent factors in cable driven robot dynamics that can affect the precision and accuracy of the robot. These factors include pulley design, cable properties such as material, elongation and mass, and the estimation of the feasible workspace of the robot [15].

As seen in the previous figures, horizontal movements present more errors than vertical. This can be explained due to fact that the motors are not completely synchronized as shown 3.3.4. This time gap between both motors has greater influences on movements requiring both motors to move in the same direction than on those requiring opposite movements. Also, gravity acts as an orthogonal force in horizontal movements which causes undesired behaviors in the cables.

5. Conclusions

Regarding the calculation of the robot's workspace, two fundamental factors are derived for its optimization, the minimum tension factor and the maximum tension. Analyzing the complexity of optimizing both parameters simultaneously one can opt to leave one of these parameters as input (fixed) and calibrate the other. Finally, maximum torque was optimized because it was found that the security factor can be personalized according to the application or scenario in which the robot is going to operate.

The maximum torque calculated using the workspace only takes into consideration static effects. This condition restricts the veracity of the calculation and makes it valid for small speeds and accelerations where the dynamic effects are negligible.

When evaluating motor synchronization, the obtained results were considered satisfactory because both motors were adjusted with the design of one controller.

The use of high-order trajectories is fundamental in these types of applications. Ensuring smooth speeds and acceleration curves causes actuators to make low efforts that do not compromise the mechanical design of the robot.

When transitioning from simulations to the prototype, robot precision and accuracy was smaller than in the simulations. This is because the mechanical components of the robot influence the control of the motors causing the actuator not to move in a linear way and have millimetric errors in its Cartesian position. One of these mechanical factors is the backlash between the threaded shaft and the drum of the cable collection mechanism. In addition, it has been shown [7], that changing the shape of the end effector for one that includes fixed pulleys of the same radius as the pulleys of the structure, significantly improves robot movement.

References

[1] Bosscher, P., et al. Cable-suspended robotic contour crafting system, Automation in Construction, 17(1), pp. 45-55, 2007. DOI: 10.1016/j.autcon.2007.02.011

[2] Burcio, A., Demostración de mejora cinemática para el posicionamiento de robots comandados mediante cables, BSc. Eng. Thesis, Department of Industrial Engineering, Castilla- La Mancha University, Toledo, Spain, 2015.

[3] Garrido, J., Diseño de un robot 3D comandado por cables a partir de un modelo cartesiano convencional, BSc. Eng. Thesis, Department of Industrial Engineering, Castilla- La Mancha University, Ciudad Real, Spain, 2015.

[4] Kawamura, S., et al., Development of an ultrahigh speed robot FALCON using wire drive systems, Journal of the Robotic Society of Japan, 15(1), pp. 82-89, 1997. DOI: 10.7210/jrsj.15.82

[5] Tang, X., An overview of the development for cable-driven parallel manipulator, Advances in Mechanical Engineering, 6, 2015. DOI: 10.1155/2014/823028

[6] Dallej, T., et al., Towards vision-based control of cable-driven parallel robots, Proceedings of 2011 IEEE/RSJ International Conference on Intelligent Robots and Systems, [online]. 2011, pp. 2855-2860. Available at: https://ieeexplore.ieee.org/abstract/document/6094591/
[7] Magán, A., Robot paralelo comandado mediante cables de 4 grados de libertad, BSc. Eng. Thesis, Department of Industrial Engineering, Castilla- La Mancha University, Toledo, Spain, 2015.
[8] Barrientos, A., Fundamentos de robótica., Madrid, McGraw-Hill, 2007.
[9] Pololu.com. (2018). Pololu - 70:1 Metal Gearmotor 37Dx54L mm with 64 CPR Encoder (No End Cap). [online]. Available at: https://www.pololu.com/product/1445
[10] Castillo, F., Video Conferencia. [online]. 2016. Available at: http://enlinea.eia.edu.co/player.php?media=/multimedia/otros/seminario_congreso_ciima_1 [Accessed 1 Aug. 2016].
[11] Dorf, R. and Bishop, R., Modern control systems, 12th ed., Estados Unidos, Prentice Hall, 2011.
[12] I. National Instruments, User Guide and Specifications Ni myRIO-1900 [online]. Available at: http://www.ni.com/pdf/manuals/376047d.pdf
[13] Mathworks, Matlab® 2017. [Online]. Available at: https://es.mathworks.com/products/matlab.html.
[14] Álvarez, C., Soto, A. and Watkins, F., Simulación de controladores digitales, Ingeniare. Revista Chilena de Ingeniería, 17(3), pp. 309-316, 2009. DOI: 10.4067/S0718-33052009000300004
[15] Schmidt, V., Modeling techniques and reliable real-time implementation of kinematics for cable-driven parallel robots using polymer fiber cables, Ph.D Dissertation, Faculty of Design, Production and Vehicle Technology, Universität Stuttgart, Stuttgart, Germany, 2017.
[16] Wei, H., Qin, Y. and Su, Y., Motion control strategy and stability analysis for high-speed cable-driven camera robots with cable inertia effects, International Journal of Advanced Robotic Systems, pp. 1-14, 2016. DOI: 10.1177/1729881416663374
[17] Melchiorri, C., Trajectory planning for robot manipulators, Universit`a di Bologna, 2008. [Online]. Available at: http://www-lar.deis.unibo.it/people/cmelchiorri/Files_Robotica/RIM_09_Traj.pdf
[18] Florez, D., Castro, F. y Castillo, R., Planeación y ejecución de trayectorias en robot delta, Universidad Militar Nueva Granada, 2014. DOI: 10.22517/23447214.11241.
[19] OSP and ComPADRE. Tracker video analysis and modeling tool, 2017. [Online]. Available at: http://physlets.org/tracker/

J.P. Castrillón-Restrepo, is graduated from Universidad EIA, Colombia with a BSc. Eng in Mechatronics Engineering. His bachelor thesis, developed alongside Federico Saldarriaga, explores the implementation of a cable driven planar robot in logistics applications.in 2017, he did an internship in "AKT Motos", developing various mechatronics projects including a pick to light system. He has also participated in the "Motors, Thermal Machines and Automotive Motion" seedbed research group in Universidad EIA.
ORCID: 0000-0002-7832-1344

S. Jiménez-Gómez was born in Medellin - Colombia in 1987. He obtained the BSc. degree of Mechatronic Engineer in 2011 and the MSc. degree in Mechatronics in 2013, both from the Militar Nueva Granada University, Bogota-Colombia. He had an honor distinction for his master thesis called Design and assembly of an experimental setup for characterization and testing of Magneteorheological dampers. Currently he is part of the Department of Automatic and Robotics and is lecturer in control and automation subjects at EIA University, Colombia. His research interest is focused on identification and control of electro-mechanical systems.
ORCID: 0000-0003-3047-8809

F. Saldarriaga-Ángel, has participated in the "Drones & UAVs" seedbed research group in Universidad EIA, Colombia. In 2017, he did an internship in "Avianca" where he focused on projects based on Lean 6 sigma methodology. Graduated from EIA University Colombia, he finished a BSc. in Eng in Mechatronics Engineering in 2017. His bachelor thesis, developed alongside Juan Pablo Castrillón, explores the implementation of a cable driven planar robot in logistics applications.
ORCID: 0000-0001-9420-9742